Photonic detection and characterization of DNA using sapphire microspheres

Mohammed Sharif Murib
Weng-Siang Yeap
Daan Martens
Peter Bienstman
Ward De Ceuninck
Bart van Grinsven
Michael J. Schöning
Luc Michiels
Ken Haenen
Marcel Ameloot
Ali Serpengüzel
Patrick Wagner

SPIE.

Photonic detection and characterization of DNA using sapphire microspheres

Mohammed Sharif Murib,[a] Weng-Siang Yeap,[a] Daan Martens,[b] Peter Bienstman,[b] Ward De Ceuninck,[a,c] Bart van Grinsven,[a,c] Michael J. Schöning,[d] Luc Michiels,[e] Ken Haenen,[a,c] Marcel Ameloot,[e] Ali Serpengüzel,[f] and Patrick Wagner[a,c,*]

[a]Hasselt University, Instituut voor Materiaalonderzoek, Wetenschapspark 1, B-3590 Diepenbeek, Belgium
[b]Ghent University—Information Technology, Department of Information Technology, Photonics Research Group, Sint-Pietersnieuwstraat 41, B-9000 Gent, Belgium
[c]Interuniversitair Microelectronica Centrum vereniging zonder winstoogmerk, Division Instituut voor Materiaalonderzoek in de Micro-Elektronica, Wetenschapspark 1, B-3590 Diepenbeek, Belgium
[d]Aachen University of Applied Sciences, Institute of Nano- and Biotechnologies, Heinrich-Mußmann-Straße 1, D-52428 Jülich, Germany
[e]Hasselt University, BIOMED, Agoralaan Building C, B-3590 Diepenbeek, Belgium
[f]Koç University, Department of Physics, Microphotonics Research Laboratory, Rumelifeneri Yolu, Sarıyer, Istanbul 34450, Turkey

Abstract. A microcavity-based deoxyribonucleic acid (DNA) optical biosensor is demonstrated for the first time using synthetic sapphire for the optical cavity. Transmitted and elastic scattering intensity at 1510 nm are analyzed from a sapphire microsphere (radius 500 μm, refractive index 1.77) on an optical fiber half coupler. The 0.43 nm angular mode spacing of the resonances correlates well with the optical size of the sapphire sphere. Probe DNA consisting of a 36-mer fragment was covalently immobilized on a sapphire microsphere and hybridized with a 29-mer target DNA. Whispering gallery modes (WGMs) were monitored before the sapphire was functionalized with DNA and after it was functionalized with single-stranded DNA (ssDNA) and double-stranded DNA (dsDNA). The shift in WGMs from the surface modification with DNA was measured and correlated well with the estimated thickness of the add-on DNA layer. It is shown that ssDNA is more uniformly oriented on the sapphire surface than dsDNA. In addition, it is shown that functionalization of the sapphire spherical surface with DNA does not affect the quality factor ($Q \approx 10^4$) of the sapphire microspheres. The use of sapphire is especially interesting because this material is chemically resilient, biocompatible, and widely used for medical implants. © 2014 Society of Photo-Optical Instrumentation Engineers (SPIE) [DOI: 10.1117/1.JBO.19.9.097006]

Keywords: deoxyribonucleic acid; label-free biosensor; microcavity; photonics; quality factor; sapphire microsphere; whispering gallery modes.

Paper 140320RR received May 21, 2014; revised manuscript received Sep. 2, 2014; accepted for publication Sep. 3, 2014; published online Sep. 26, 2014.

1 Introduction

There is a growing demand for sensors to detect nanoparticles, viruses,[1] and biomolecules[2] because of the recent advances in nanotechnology and biology. Especially, clinical diagnostics demands sensitive real-time- and label-free detection techniques.[3] Biomolecules recognition and deoxyribonucleic acid (DNA) denaturation were studied by different types of measurement setups such as microfluidic sensing,[4] elastic measurements at the level of a single molecule,[5] force-induced denaturation,[6] and by monitoring the denaturation dynamics in real time using impedance spectroscopy.[7] Other label-free biosensors that have been shown recently are nanowires,[8] nanoparticle probes,[9] biochips,[10] mechanical cantilevers,[11] and field-effect sensors.[12] Label-free optical biosensors offer great advantages over more conventional analytical techniques.[13] This is related to the fact that optical biosensors are highly sensitive, fast, reproducible, and circumvent the need to modify target molecules by labeling.[3,13]

Optical biosensors are powerful transducers that can detect the presence of (bio)chemical molecules at a surface as well as physical properties of the medium.[14] For example, in their seminal work, Arnold et al. demonstrated protein adsorption in spherical photonic microcavities.[15] Zlatanovic et al. demonstrated the detection of the presence and concentration of proteins in a physiological buffer using photonic crystal microcavities.[3] Optical biosensors are insensitive to electromagnetic interference, capable of performing remote sensing, and can provide multiplexed detection within a single device.[16] Also, optical biosensors can be extremely sensitive (nanomolar concentrations or less), nondestructive to the sample, and the transduction processes in optical biosensors generally takes place at a surface and can be tailored to sense almost any kind of molecule, chemical and biological.[17]

Optical sensing can be performed using ring resonators,[18] confocal microscopy,[7] prism couplers,[19] spherical cavities,[20] and fiber-optic waveguides.[21] In ring resonators, spherical cavities, and fiber-optics waveguides, the light is coupled through the waveguides, and an evanescent field extends beyond the waveguide surface by ≈100 nm.[18] The analytes bound to the surfaces of these waveguides will lie in the path of the evanescent field, and as a result, they change the effective size and refractive index of the guided mode.[18] Optical sensing using confocal microscopy and fiber-optic waveguides have certain disadvantages. For example, fiber-optics waveguide sensors are typically quite long. In order to achieve a high signal and low detection limit, the waveguide must be on the order of a few centimeters

*Address all correspondence to: Patrick Wagner, E-mail: Patrick.Wagner@uhasselt.be

long, because the sensing signal is accumulated along the waveguide.[18] Confocal microscopy requires fluorescent labeling for detection, which is time-consuming, complex, and may not always be suitable for rapid biophysical and routine characterization tasks.[22] In addition, real-time hybridization monitoring using confocal microscopy cannot be performed, because it is hard to distinguish between unbound targets in solution and those that have been hybridized to the probe on the surface, as both will fluoresce when imaged.[23]

Photonic microcavities such as circular resonators or spherical resonators are promising optical label-free detection setups.[20,24] In a photonic microcavity, the target molecules are sampled hundreds of times because of the recirculation of light within the microcavity by total internal reflection (TIR).[24] The target molecules induce a change in the optical microcavity properties such as the size and refractive index; and as a result, a change in the whispering gallery mode (WGM) resonant wavelength is encountered.[25] Recently, a silicon-on-insulator (SOI) microring resonator for sensitive label-free biosensing was fabricated.[26] After coating with biotin receptor molecules, a detection limit of 0.37 fg avidin mass (3260 molecules) was shown.[27,28]

In this article, an experimental study of an optical biosensor concept based on elastic light scattering from sapphire microspheres is performed. The sapphire microsphere surface was functionalized with DNA layers, and the corresponding shift of WGMs was monitored and analyzed. Sapphire shows outstanding chemical inertness, wear resistance, and biocompatibility.[29] Hence, it is widely used for implants such as hip implants,[29] dental implants,[30] and endosseous implants.[31] Moreover, its wide optical transmission band from the ultraviolet to the near-infrared (near-IR)[32] suggests application potential in optical biosensors. So far, SOI ring resonators[26] and glass microspheres[20] have been used as microcavity-based biosensors. The degradation of silicon and glass interfaces in aqueous solutions limits their use as biosensors,[33,34] and therefore, we consider synthetic sapphire as a promising alternative.

2 Sapphire Sphere Modification with Double-Stranded DNA

Probe DNA consisting of a 36-mer fragment was covalently immobilized on a sapphire sphere and hybridized with 29-mer target DNA. The base sequences of the probe and target DNA are given in Table 1. These fragment lengths comply well with typical lengths used in the commercially available DNA microarray platforms. Experiments with other sizes of DNA oligonucleotides would enrichen the measurement database and enhance the robustness of the measurement method. The sapphire sphere (Edmund Optics) was ultrasonically cleaned in acetone, ultrapure water (Sartorius Stedim Biotech Ultra Pure Water System Type 1), and isopropanol for 20 min in each

Table 1 Base sequences of the probe DNA and the corresponding full match DNA.

Name	Sequence
Probe DNA	5′-COOH-AAAAAAACCC CTG CAG CCC ATG TAT ACC CCC GAA CC-3′
Full match	5′-FAM-488-GGT TCG GGG GTA TAC ATG GGC TGC AGG GG-3′

bath. Next, it was immersed in 10 mM HNO_3 solution at room temperature for 30 min to create OH groups on the surface.[35,36] Afterward, the sapphire sphere was rinsed with ultrapure water and dried with flowing nitrogen gas.

Silanization of the sapphire samples was carried out by liquid phase deposition of a solution of silane in an organic solvent.[37] The samples were placed in a 600 mM solution of (3-aminopropyl)triethoxysilane (APTES, 99%; Sigma-Aldrich, St. Louis, Missouri) in toluene (≥ 99.9%, Sigma-Aldrich) for 15 h in a nitrogen-filled glovebox. To wash off the unbound APTES, the samples were first rinsed with toluene, followed by tetrahydrofuran (≥ 99.9%, Sigma-Aldrich). After drying the samples in a nitrogen stream, they were cured for 2 h at 150°C. Curing at this high temperature will create a much stronger film of APTES on the surface.[37] This silanization step creates an amine-modified surface.[38] The zero-length crosslinker, 1-ethyl-3-[3-dimethylaminopropyl]-carbodiimide was used for the covalent coupling of the 5′ side of a carboxyl-modified 36-mer single-stranded DNA (ssDNA) fragment to the amine-modified surface in 2-[N-morpholino]-ethannesulphonic acid buffer at 4°C. In a following step, 6 μl 6-fluorescein amidite (FAM)-488-modified DNA was mixed with 14 μl 1× polymerase chain reaction buffer and added to the ssDNA-modified sapphire sphere. The FAM-488 dye allows us to confirm the presence of double-stranded DNA (dsDNA) by confocal microscopy. The sphere was then incubated at 35°C for 2 h. Nonspecifically bound DNA was removed using a double washing step. In a first step, the sphere was washed with 2× saline sodium citrate (SSC) +0.5% sodium dodecyl sulphate for 30 min. Next, the sphere was washed twice with 0.2× SSC at 30°C for 5 min. Finally, the sphere was rinsed with phosphate-buffered saline (PBS) of pH 7.2 and stored in PBS at 4°C.[33]

3 Confocal Fluorescence Microscopy

Fluorescence images were taken on a Zeiss, Jena, Germany LSM 510 META Axiovert 200 M laser scanning confocal fluorescence microscope to confirm the dsDNA covalent binding to the sapphire microsphere (Fig. 1). To excite the FAM-488 fluorescence dye, a 488 nm argon-ion laser was used with a maximum intensity at the sample surface of 30 μW, in order to avoid
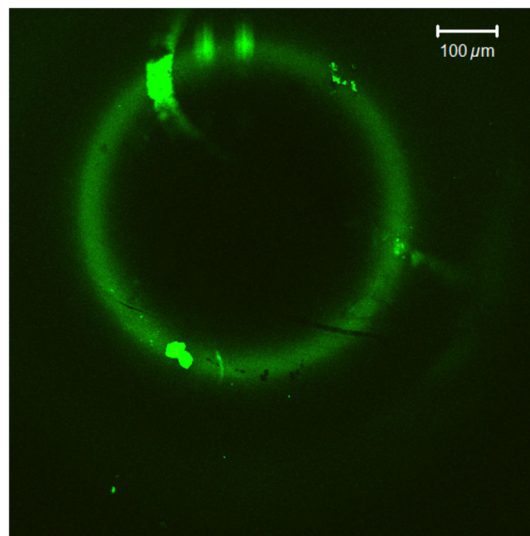

Fig. 1 Confocal fluorescence image of a sapphire microsphere where the binding protocol was carried out as described in Sec. 2.

bleaching during the image acquisition. The fluorescence emission was collected using a 505-nm long-pass filter. The image was collected with a $10 \times /0.3$ Plan Neofluar air objective with a working distance of 5.6 mm. The following filter sets were used: MBS HFT 488, DBS NFT 490, or mirror. The image size was 900×900 μm^2. The pinhole size was 150 μm, and the laser intensity was set at 10%. The detector gain, being a measure for the photomultiplier voltage in arbitrary units, was set to 950.

4 Photonic Detection Mechanism

The electromagnetic wave can be trapped inside the sapphire sphere by almost TIR,[39] and it evanesces partially into the surrounding medium.[24] As a result, the light will interact with the molecules once they are captured on the surface on resonance.[24] The electromagnetic wave circumnavigates the sphere and returns back to its initial point in phase.[39] A periodic circumnavigating wave in the sphere produces a series of sharp peaks of WGMs as a function of the size parameter $x = 2\pi a N/\lambda$, where a is the sphere radius, λ is the wavelength of the laser in vacuum, and N is the refractive index of the surrounding medium [Fig. 1(a)].[39] A tunable diode laser (DL; Santec TSL 510, Komaki, Aichi, Japan) with a wavelength of 1510 nm was used in order to excite the WGMs of the sapphire microsphere, through a single-mode optical fiber (Evanescent Optics Inc., Burlington, Ontario, Canada), which couples >97% of the light passing through the coupler to an overlay index matching [Fig. 2(a)]. The DL was tuned from 1510 to 1512 nm with a step

size of 5 pm. The elastically scattered light from the sapphire microsphere at 90 deg was collected by a two-channel optical microscope and detected by a germanium (Ge) photodiode (D1). The Ge photodiode signal was sent to a digital storage oscilloscope for signal monitoring and data acquisition. The transmitted power through the optical fiber was detected by a second photodiode (D2) connected to the optical multimeter. All the optoelectronic equipments were controlled using the general purpose interface bus standard.

The system was modeled using the Generalized Lorenz–Mie Theory, which describes the electromagnetic scattering of an arbitrary light beam by a spherical microparticle.[41] The elastic scattering intensity from the sphere and transmittance intensity at the output of the optical fiber for transverse electric and transverse magnetic polarization were calculated for sapphire spheres before and after surface modifications with biomolecules.[40] Figure 2(b) shows a schematic of WGMs (λ_1 and λ_2) of same radial mode order and consecutive polar angular mode number, and the shift of WGMs from the sphere's surface modification. The mode spacing ($\Delta\lambda$) is the spectral range between resonances having the same radial mode order (the number of maxima between the center and the radius a in the radial direction in the intensity distribution of the mode) and consecutive polar mode number (the number of maxima between 0 and 180 deg polar angle in the intensity distribution of the mode). The mode spacing $\Delta\lambda$ can be calculated using[41]
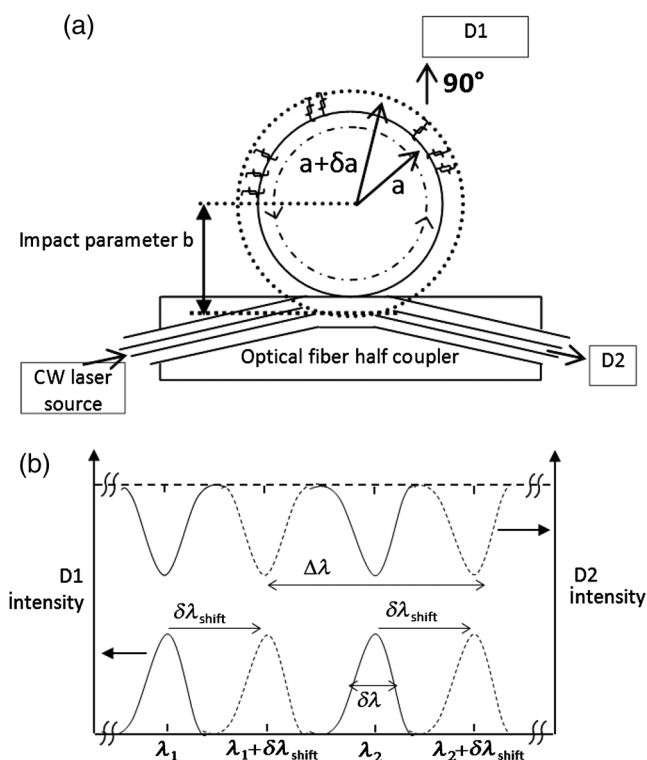

Fig. 2 Schematic geometry of the microsphere with a biologically modified surface coupled to a half coupler optical fiber. (b) Schematic illustration of whispering gallery modes (WGMs; λ_1 and λ_2) of same radial mode order and consecutive polar angular mode number and the expected shift of the WGMs from the sphere's surface modification.[40] $\Delta\lambda$ is the mode spacing of resonances having the same radial mode order and consecutive polar angular mode number. $\delta\lambda_{shift}$ is the wavelength shift due to the spheres surface modification by the adsorbed molecules.
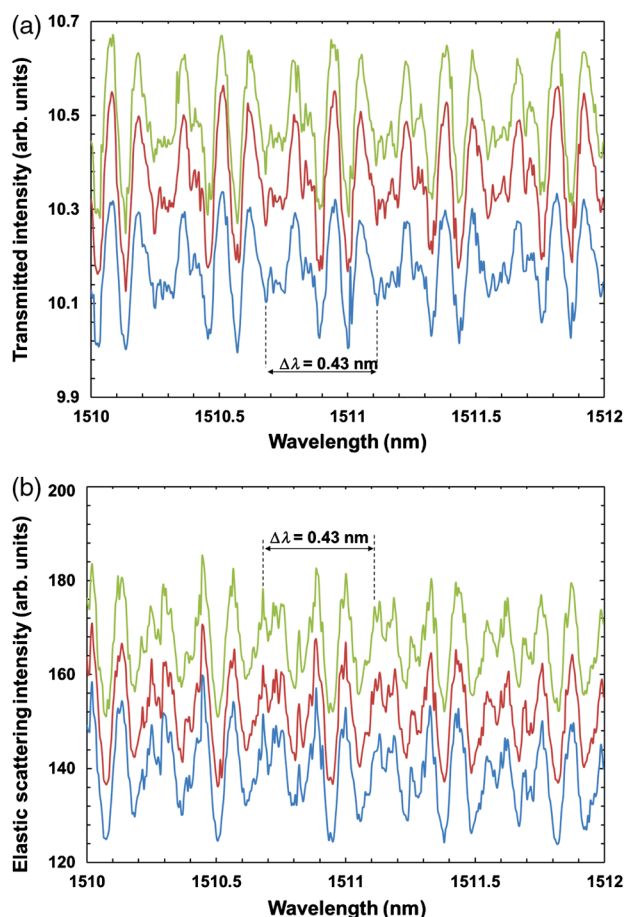

Fig. 3 Transmitted intensity (a) and elastic scattering intensity (b) spectra from nonmodified sapphire sphere repeated three times in order to demonstrate the reproducibility of the concept. Spectra were offset in order to distinguish them in one graph.

$$\Delta\lambda = \frac{\lambda^2 \arctan\sqrt{m^2-1}}{2\pi a\sqrt{m^2-1}}, \quad (1)$$

where m is the relative refractive index of the sphere (refractive index of the sphere/refractive index of the surrounding medium), λ is the wavelength of the laser source in vacuum, and a is the sphere's radius.

If molecules are tethered onto the sphere's surface, these molecules will induce a change of the optical properties of the sphere such as its effective size and refractive index near the surface of the sphere proportional to the amount of bound molecules.[24] As a result, the resonance wavelength will change further and result in the phenomenon of resonant shift as shown by the dashed lines in Fig. 1(b).[24] The wavelength shift $\delta\lambda_{\text{shift}}$ can be calculated by

$$\frac{\delta\lambda_{\text{shift}}}{\lambda} = \frac{\delta a}{a}, \quad (2)$$

where δa is the change in sphere radius because of the interaction between the adsorbed molecules.[25]

5 Experimental Results

In order to ensure the stability and reproducibility of the resonances, the experiment was repeated at least three times with nonmodified 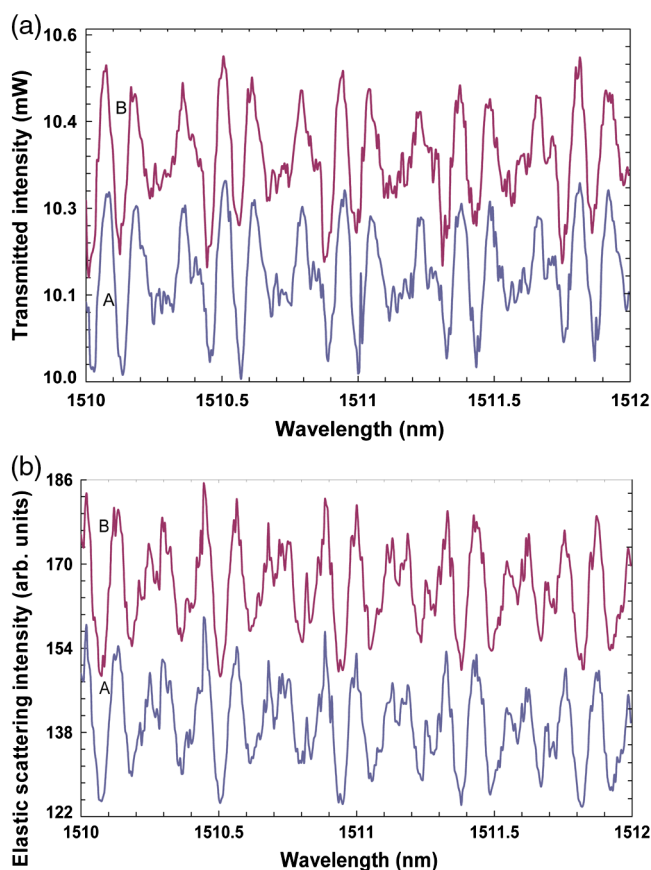and modified sapphire spheres in air. The same sphere was used in all the measurements. Figure 3 represents the three repeated spectra for the transmitted intensity (a) and the elastic scattering intensity (b) from the nonmodified sapphire sphere. As a result, the resonances were proven to be repeatable and stable because they are well overlapping. The $\Delta\lambda$ of the WGMs is observed to be 0.432 nm, which is comparable with the $\Delta\lambda = 0.482$ nm estimated using Eq. (1) for a 1-mm diameter sapphire microsphere with a refractive index of 1.77. The slight discrepancy can possibly be attributed to minor uncertainties in the size, ellipticity, and the refractive index of the sphere. For each maximum in the elastic scattering spectrum, there is a corresponding minimum in the transmittance spectrum. The minima in the transmittance spectrum correspond to an amount of light coupled from the fiber into the sphere. From the comparison of the transmission spectrum in the absence of the microsphere (not shown) to the transmission spectra with the microsphere, the coupling from the fiber to the sphere is estimated to be on the order of 3%.

The next step was to investigate what would happen if the sphere was moved around the initial coupling point and then returned back to almost the same position. As shown in Fig. 4, the resonance positions are overlapping again, but their intensities have slightly changed because of the change in the coupling angle. Within the experimental resolution, the spectral locations of the peaks and minima are identical to those represented in Fig. 3, supporting the high reproducibility of the described method.
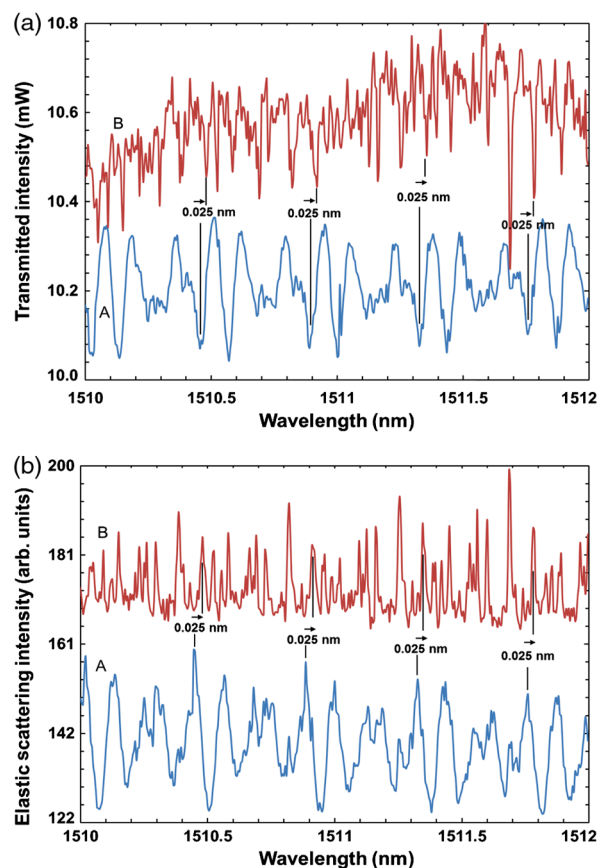

Fig. 4 Transmitted intensity (a) and elastic scattering intensity (b) spectra from nonmodified sapphire sphere repeated twice. (A) Sphere initially on the coupler. (B) Sphere was raised over the coupler and moved around the initial coupling point and then returned back to almost the same initial coupling point.

Fig. 5 Transmitted intensity (a) and elastic scattering intensity (b) spectra from sapphire sphere modified with ssDNA and the corresponding shift. (A) Nonmodified sphere. (B) Sphere modified with the ssDNA.

Then, the shift in WGMs of the sapphire microsphere from the surface functionalization with ssDNA was measured. The transmitted and the elastic scattering intensity spectra in the wavelength range from 1510 to 1512 nm are shown in Figs. 5(a) and 5(b), respectively.

As can be clearly seen from Figs. 5(a) and 5(b), the resonances are red-shifted by 0.025 nm, which corresponds to a size shift of 8.3 nm as calculated using Eq. (2). In a previous ellipsometric study, we found that the film thickness of the 36 base pairs ssDNA layer was about 7.6 nm with a surface roughness of 0.7 nm on nanocrystalline diamond.[42] This correlates well with the 8.3 nm size shift measured with the microsphere resonator here.

After the hybridization with the target DNA (100 μM), the resonances were red-shifted by 0.03 nm, which corresponds to a radius increase of 10 nm, as calculated using Eq. (2). The transmitted and the elastic scattering intensity spectra are shown in Figs. 6(a) and 6(b), respectively.

The layer of 29 base pairs dsDNA amounts to a film thickness of about 10.8 nm and a surface roughness of 1.7 nm on nanocrystalline diamond.[42] This again correlates well with the size shift value measured in this setup. The average mass density for the probe DNA onto the sphere surface was estimated to be about 29 ng/mm^2.[20,25] The mass of the probe DNA bound to the sphere surface was estimated to be about 0.1 μg, which

corresponds to 5.4×10^{12} ssDNA molecules (probe DNA molecular weight is 11060.3 g/mol). In addition, the observed shift corresponds to about one and one half times the resonance linewidth in the ssDNA case and about two times in the dsDNA case, which supports the possibility of identifying about one-third lower concentrations of biomolecules than what was detected in this experiment. In our case, there is a possibility of identifying about 0.1 μg of probe DNA.

The dsDNA was denatured then by 0.1 M sodium hydroxide NaOH, rinsed with ultrapure water, and dried in nitrogen gas. The transmitted intensity and the elastic scattering intensity spectra were collected again [Figs. 7(a) and 7(b)]. As expected, the resonances were blue-shifted back almost to the same position as in Figs. 5(a) and 5(b).

Now, we compare the linewidths of the resonances for ssDNA, dsDNA, and denatured dsDNA. The linewidths of the resonances for ssDNA spectra [Figs. 5(a) and 5(b)] were slightly narrower, and more resonances showed up as compared with dsDNA spectra [Figs. 6(a) and 6(b)]. This can be attributed to the fact that the surface is smoother and might be more homogeneously covered with ssDNA (surface roughness 0.7 nm)[42] than it is with dsDNA (surface roughness 1.7 nm).[42] The smoother the microcavity surface is, the higher the quality factor.[43] When the dsDNA was denatured, the linewidths remained broad [Figs. 7(a) and 7(b)]. This can be attributed
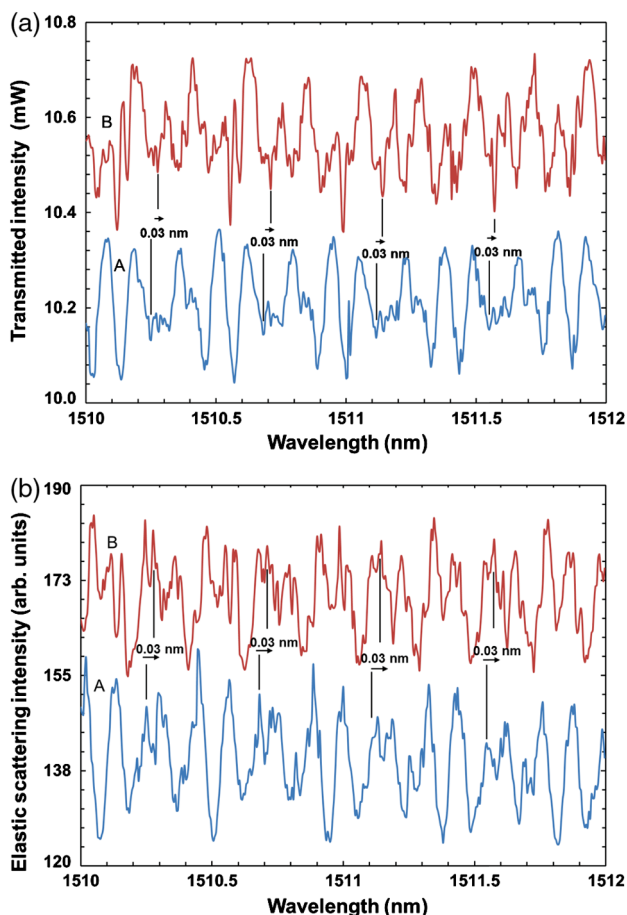

Fig. 6 Transmitted intensity (a) and elastic scattering intensity (b) spectra from sapphire sphere modified with dsDNA and the corresponding shift. (A) Nonmodified sphere. (B) Sphere modified with the dsDNA.
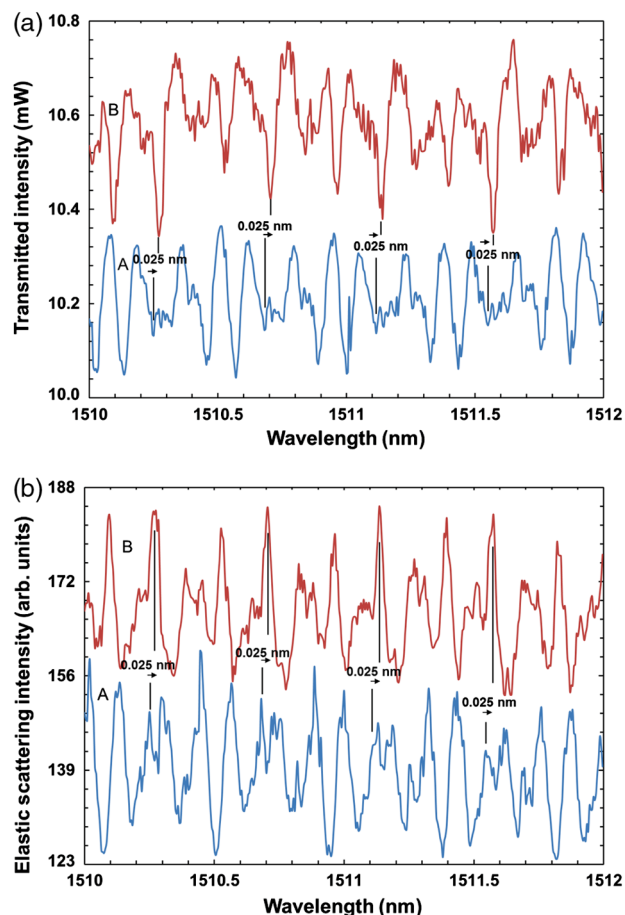

Fig. 7 Transmitted intensity (a) and elastic scattering intensity (b) spectra from sapphire sphere after dsDNA is denatured and the corresponding shift. (A) Nonmodified sphere. (B) DNA modified sphere after denaturation of dsDNA to ssDNA.

to the fact that there might be some denatured ssDNA strands still attached to the surface. This will result in a nonhomogeneous surface that scatters the photons and decreases the resonances quality factor.[43] However, the quality factor was still preserved at a high value ($Q \approx 10^4$) in all the functionalization steps except for the ssDNA ($Q \approx 10^5$) functionalization step, when more resonances showed up due to surface smoothness.

6 Conclusions

A concept for a label-free photonic biosensor was proposed with possible applications in the identification of biomolecules and in the observation of hybridization and denaturation of DNA. Elastic light scattering and transmitted intensity from sapphire spheres were measured in the wavelength range of 1500 nm. The resonance shift from the sphere-surface modification with ssDNA and dsDNA was measured and analyzed. The surface functionalization with ssDNA and dsDNA did not significantly lower the quality factor ($Q \approx 10^4$). The surface modified with ssDNA was smoother, and the ssDNA seemed to be aligned more homogeneously than the dsDNA. This resulted in more resonances in the spectrum of ssDNA than in the dsDNA. The measurements showed that an optical biosensor based on spherical cavities is a good candidate for biomolecules identification and DNA hybridization and denaturation. The shift in resonances can be analyzed from the transmission signal of the optical fiber or from the elastic scattering intensity. Furthermore, for a resonant linewidth of 0.015 nm at 1500 nm, the modified sapphire sphere had a spectral shift of about two times the resonant linewidth, which supports the possibility of identifying about 0.1 μg probe DNA. In summary, the sapphire microcavity-based sensor can be used to study the physical properties of DNA and protein molecules. All in all, we have introduced synthetic sapphire, being an established implant material, as active element in a photonic biosensor platform, allowing for future lab-on-chip bioanalytical applications. Advantages compared with silicon-based photonics are especially seen in the resilient behavior of sapphire, meaning that such a device might also operate under harsher chemical or temperature conditions.

References

1. S. Arnold et al., "MicroParticle photophysics illuminates viral bio-sensing," *Faraday Discuss.* **137**, 65–83 (2008); F. Vollmer, S. Arnold, and D. Keng, "Single virus detection from the reactive shift of a whispering-gallery mode," *Proc. Natl. Acad. Sci. U. S. A.* **105**(52), 20701–20704 (2008).
2. N. Lagos and M. M. Sigalas, "Single particle detection in a system of two microdisks," *Sens. Actuators B* **153**(1), 252–255 (2011).
3. S. Zlatanovic et al., "Photonic crystal microcavity sensor for ultracompact monitoring of reaction kinetics and protein concentration," *Sens. Actuators B* **141**(1), 13–19 (2009).
4. J. Wu and M. Gu, "Microfluidic sensing: state of the art fabrication and detection techniques," *J. Biomed. Opt.* **16**(8), 080901 (2011).
5. T. Strick et al., "Twisting and stretching single DNA molecules," *Prog. Biophys. Mol. Biol.* **74**(1–2), 115–140 (2000).
6. U. Bockelmann et al., "Unzipping DNA with optical tweezers: high sequence sensitivity and force flips," *Biophys. J.* **82**(3), 1537–1553 (2002).
7. B. van Grinsven et al., "Rapid assessment of the stability of DNA duplexes by impedimetric real-time monitoring of chemically induced denaturation," *Lab Chip* **11**(9), 1656–1663 (2011).
8. Q. Wang et al., "Non-enzymatic glucose sensing on long and short diamond nanowire electrodes," *Electrochem. Commun.* **34**, 286–290 (2013).
9. J. M. Nam, C. S. Thaxton, and C. A. Mirkin, "Nanoparticle-based bio-bar codes for the ultrasensitive detection of proteins," *Science* **301**(5641), 1884–1886 (2003).
10. W. S. Yeo et al., "Label-free detection of protein–protein interactions on biochips," *Angew. Chem. Int. Ed.* **44**(34), 5480–5483 (2005).
11. T. P. Burg et al., "Weighing of biomolecules, single cells and single nanoparticles in fluid," *Nature* **446**(7139), 1066–1069 (2007).
12. A. Poghossian et al., "Field-effect sensors with charged macromolecules: characterisation by capacitance-voltage, constant-capacitance, impedance spectroscopy and atomic-force microscopy methods," *Biosens. Bioelectron.* **22**(9–10), 2100–2107 (2007); S. Ingebrandt et al., "Label-free detection of single nucleotide polymorphisms utilizing the differential transfer function of field-effect transistors," *Biosens. Bioelectron.* **22**(12), 2834–2840 (2007).
13. D. Dey and T. Goswami, "Optical biosensors: a revolution towards quantum nanoscale electronics device fabrication," *J. Biomed. Biotechnol.* **2011**, 348218 (2011); R. Narayanaswamy and O. S. Wolfbeis, *Optical Sensors, Industrial, Environmental, and Diagnostic Applications*, Springer-Verlag, Berlin (2004).
14. A. Serpengüzel, S. Arnold, and G. Griffel, "Excitation of resonances of microspheres on an optical fiber," *Opt. Lett.* **20**(7), 654–656 (1995); A. L. Huston and J. D. Eversole, "Strain-sensitive elastic scattering from cylinders," *Opt. Lett.* **18**(13), 1104–1106 (1993).
15. S. Arnold et al., "Shift of whispering gallery modes in microspheres by protein adsorption," *Opt. Lett.* **28**(4), 272–274 (2003); F. Vollmer et al., "Protein detection by optical shift of a resonant microcavity," *Appl. Phys. Lett.* **80**(21), 4057–4059 (2002).
16. X. D. Fan et al., "Sensitive optical biosensors for unlabeled targets: a review," *Anal. Chim. Acta* **620**(1–2), 8–26 (2008).
17. J. L. Nadeau et al., "High-Q whispering-gallery mode sensor in liquids," *Proc. SPIE* **4629**, 172–180 (2002).
18. J. D. Suter et al., "Label-free quantitative DNA detection using the liquid core optical ring resonator," *Biosens. Bioelectron.* **23**(7), 1003–1009 (2008).
19. Z. B. Bahşi et al., "A novel label-free optical biosensor using synthetic oligonucleotides from E. coli O157:H7: elementary sensitivity tests," *Sensors* **9**(6), 4890–4900 (2009).
20. M. Baaske and F. Vollmer, "Optical resonator biosensors: molecular diagnostic and nanoparticle detection on an integrated platform," *Chem. Phys. Chem.* **13**(2), 427–436 (2012).
21. V. M. N. Passaro et al., "Guided-wave optical biosensors," *Sensors* **7**(4), 508–536 (2007); J. P. Golden et al., "An evanescent-wave biosensor. II. Fluorescent signal acquisition from tapered fiber optic probes," *IEEE Trans. Biomed. Eng.* **41**(6), 585–591 (1994).
22. A. Q. Liu et al., "Label-free detection with micro optical fluidic systems (MOFS): a review," *Anal. Bioanal. Chem.* **391**(7), 2443–2452 (2008).
23. P. M. Levine et al., "Real-time, multiplexed electrochemical DNA detection using an active complementary metal-oxide-semiconductor biosensor array with integrated sensor electronics," *Biosens. Bioelectron.* **24**(7), 1995–2001 (2009).
24. F. Vollmer et al., "Multiplexed DNA quantification by spectroscopic shift of two microsphere cavities," *Biophys. J.* **85**(3), 1974–1979 (2003).
25. F. Vollmer and S. Arnold, "Whispering-gallery-mode biosensing: label-free detection down to single molecules," *Nat. Methods* **5**(7), 591–596 (2008).
26. K. De Vos et al., "Silicon-on-insulator microring resonator for sensitive and label-free biosensing," *Opt. Express* **15**(12), 7610–7615 (2007).
27. R. Kirchner et al., "Chemical functional polymers for direct UV assisted nanoimprinting of polymeric photonic microring resonators," *Phys. Status Solidi A* **208**(6), 1308–1314 (2011).
28. K. De Vos et al., "SOI optical microring resonator with poly(ethylene glycol) polymer brush for label-free biosensor applications," *Biosens. Bioelectron.* **24**(8), 2528–2533 (2009).

29. A. G. Mamalis et al., "A novel concept for the manufacture of individual sapphire-metallic hip joint endoprostheses," *Biol. Phys. Chem.* **6**(3), 113–117 (2006).
30. T. Takahashi et al., "Long-term observation of porous sapphire dental implants," *Bull. Tokyo Dent. Coll.* **49**(1), 23–27 (2008).
31. M. R. Rieger et al., "Alternative materials for three endosseous implants," *J. Prosthet. Dent.* **61**(6), 717–722 (1989).
32. G. Q. Zhou et al., "Ø 140 mm sapphire crystal growth by temperature gradient techniques and its color centers," *Mater. Lett.* **60**(7), 901–904 (2006).
33. V. Vermeeren et al., "Topographical and functional characterization of the ssDNA probe layer generated through EDC-mediated covalent attachment to nanocrystalline diamond using fluorescence microscopy," *Langmuir* **24**(16), 9125–9134 (2008).
34. T. Strother et al., "Synthesis and characterization of DNA-modified silicon (111) surfaces," *J. Am. Chem. Soc.* **122**(6), 1205–1209 (2000).
35. J. P. Fitts et al., "Electrostatic surface charge at aqueous/alpha-Al_2O_3 single-crystal interfaces as probed by optical second-harmonic generation," *J. Phys. Chem. B* **109**(16), 7981–7986 (2005).
36. J. H. Sung et al., "Surface structure of protonated R-sapphire ($1\bar{1}02$) studied by sum-frequency vibrational spectroscopy," *J. Am. Chem. Soc.* **133**(11), 3846–3853 (2011).
37. E. T. Vandenberg et al., "Structure of 3-aminopropyl triethoxy silane on silicon-oxide," *J. Colloid Interface Sci.* **147**(1), 103–118 (1991).
38. K. van der Maaden et al., "Fluorescent nanoparticle adhesion assay: a novel method for surface pK(a) determination of self-assembled monolayers on silicon surfaces," *Langmuir* **28**(7), 3403–3411 (2012).
39. B. R. Johnson, "Theory of morphology-dependent resonances—shape resonances and width formulas," *J. Opt. Soc. Am. A* **10**(2), 343–352 (1993).
40. M. S. Murib et al., "Analysis of an optical biosensor based on elastic light scattering from diamond-, glass-, and sapphire microspheres," *Phys. Status Solidi A* **209**(9), 1804–1810 (2012).
41. M. L. Gorodetsky, A. A. Savchenkov, and V. S. Ilchenko, "Ultimate Q of optical microsphere resonators," *Opt. Lett.* **21**(7), 453–455 (1996).
42. S. Wenmackers et al., "Structural and optical properties of DNA layers covalently attached to diamond surfaces," *Langmuir* **24**(14), 7269–7277 (2008).
43. D. W. Vernooy et al., "High-Q measurements of fused-silica microspheres in the near infrared," *Opt. Lett.* **23**(4), 247–249 (1998).

Mohammed Sharif Murib received his BSc degree in physics from Lebanese University Hadath in 2005. He received his MSc degree in physics from Koç University in 2009, where he worked with professor A. Serpengüzel at the Microphotonics Research Laboratory on elastic light scattering from microspheres. He received his PhD degree from Hasselt University in 2014, where he worked in the BIOSensor Group at the Institute for Materials Research with Prof. P. Wagner on bioelectronics and biophotonic sensors.

Weng-Siang Yeap obtained his MSc degree at National University of Singapore in 2009 and is presently a PhD student in the Wide-Bandgap Materials Group of Prof. K. Haenen within the Institute for Materials Research at Hasselt University. His research interests include the surface functionalization of diamond, diamond electrochemistry, and (bio)chemical sensors. He is the author and coauthor of several research articles in these areas.

Daan Martens received his master's degree in engineering physics from Ghent University in 2012. Since 2012, he has been working toward his PhD degree with the Photonic Research Group, Ghent University, where he is involved in the Pocket Project. His current research interests include integrated photonic biosensors, the VNIR wavelength range, silicon nitride, and on-chip spectral filters.

Peter Bienstman received his PhD degree from Ghent University, Belgium, in 2001, at the Department of Information Technology, where he is currently an associate professor. During 2001 to 2002, he spent a year in the Joannopoulos research group at MIT. His research interests include several applications of nanophotonics (biosensors, photonic information processing) as well as nanophotonics modeling. He has been awarded an ERC starting grant for the Naresco-project: Novel Paradigms for Massively Parallel Nanophotonic Information Processing.

Ward De Ceuninck obtained his PhD degree at the former Limburgs Universitair Centrum in 1990 where he was leader of the Electrical Characterization and Reliability Group. From 2003 on, he joined IMEC where he was active in different reliability research programs and holds many related patents. Currently, he is also a professor at Hasselt University, where he is active in the field of biosensors.

Bart van Grinsven received a master's degree in bioelectronics and nanotechnology from Hasselt University in 2007. Then, he was employed by TNO Eindhoven as a development engineer and returned to the BIOSensor Group of Hasselt University in 2008. He successfully defended his PhD degree in physics in 2012. After working as a postdoctoral researcher in the same group, he switched to Maastricht University, within the Maastricht Science Programme, where he now holds the position of assistant professor.

Michael J. Schöning received his PhD degree in the field of semiconductor-based microsensors for the detection of ions in liquids from Karlsruhe University of Technology in 1993. In 1999, he was appointed as full professor at Aachen University of Applied Sciences, Jülich. Since 2006, he serves as a director of the Institute of Nano- and Biotechnologies at the Aachen University of Applied Sciences. His main research subjects concern silicon-based chemical and biological sensors, thin-film technologies, solid-state physics, microsystems, and nano(bio-)technology.

Luc Michiels is a full professor of the Faculty of Medicine and Life Sciences at Hasselt University. He is responsible for the bionanotechnology research program in the Biomedical Research Institute BIOMED, and his research focuses on the integration of disease biomarkers in innovative electronic biosensing platforms for the development of new biomedical applications.

Ken Haenen obtained his PhD degree at Hasselt University on the topic of the characterization of thin phosphorus doped CVD diamond films. In 2004, he became group leader of the Wide Band Gap Materials Research Group of the Institute for Materials Research from the same university, after spending a short postdoctoral period at National Institute for Materials Science, Japan. In 2008, he was appointed as a professor in experimental physics with focus on the deposition, characterization, and use of materials including chemical vapor deposition diamond, aluminum nitride, and boron nitride.

Marcel Ameloot obtained his PhD degree at Hasselt University on the topic of nanosecond fluorescence relaxations in artificial lipid membranes. After a postdoctoral position at the Johns Hopkins University, he obtained a permanent position at Hasselt University, where he became full professor in 2000. His current research interest include advanced microfluorimetric methods and second harmonic imaging microscopy to study cell-matrix interaction, dynamics of nanoparticles in biological cells, and muscle tissues.

Ali Serpengüzel received his PhD degree from Yale University. He is currently a professor and the director of the Microphotonics Research Laboratory at Koç University. His current research focuses on silicon photonics, optical microcavities, and waveguides toward applications in optical fiber communications. Other research interests include optical spectroscopy in complex media, nanophotonics, linear and nonlinear optics, and laser diagnostics toward applications in remote sensing and combustion. He is an SPIE fellow, IEEE and OSA senior member, and Sigma-Xi member.

Patrick Wagner obtained his PhD degree in physics in 1994 at the Technical University Darmstadt for his studies on superconductors. Between 1995 and 2001, he was a postdoctoral researcher at the Catholic University Leuven focusing on magnetic oxides. In 2001, he founded the BIOSensor Group within the Institute for Materials Research at Hasselt University. His research team develops label-free sensing techniques for the detection and characterization of small molecules, proteins, nucleic acids, and circulating cells.